Fluxes of biogenic components from sediment trap deployment in circumpolar waters of the Drake Passage

Gerold Wefer*, Erwin Suess†, Wolfgang Balzer‡, Gerd Liebezeit‡, Peter J. Müller*, C. André Ungerer† & Walter Zenk‡

* Geologisches Institut, Olshausenstrasse 40–60, 2300 Kiel, FRG
† School of Oceanography, Oregon State University, Corvallis, Oregon 97331, USA
‡ Institut für Meereskunde, Düsternbrooker Weg 20, 2300 Kiel, FRG

Circumpolar surface waters dominate the circulation of the Southern Ocean and sustain one of the ocean's largest standing stocks of biomass thereby producing a significant output of biogenic components, mainly diatoms, to the bottom sediments. Generally transit of biogenic matter from the sea surface to the sea floor affects nutrient regeneration fuels benthic life and transfers signals to the sediment record[1–5]. Reliable quantification of the relationship between biological production, fractionation of skeletal and tissue components and bottom sediment accumulation depends on direct vertical flux measurements from sediment trap deployments[6–9], which have proved to be most scientifically productive[10–13]. We now present data on vertical mass fluxes from the Southern Ocean and evidence for strong biogeochemical fractionation between organic carbon-, nitrogen- and phosphorus-containing compounds, siliceous and calcareous skeletal remains, and refractory aluminosilicates.

Results are from the first deployment of sediment traps in Antarctic waters. Our traps, with a collection area of 314 cm^2 (ref. 14), were attached to a moored array located at 60°54.6′ S and 57°06.0′ W in 3,625 m of water depth for 52 days from 2 December 1980 to 25 January 1981. During that time the integrated mean primary production in the study area was 0.1 g C m^{-2} day^{-1} (ref. 15). Current and temperature observations at 400 m, 1,500 m and 3,590 m of water depth revealed some unexpected results. The upper two current meters showed a general tendency of eastward water movement, although the short time series yielded no reasonable mean current vectors. The mean temperatures recorded were 1.76 °C and 1.20 °C at 400 m and 1,500 m, respectively. In both cases the standard deviation was 0.09 °C from 5,165 individual values.

In contrast to these mid-water current observations, which characterize the southern extension of the Antarctic Circumpolar Current in the Drake Passage, an unexpectedly persistent undercurrent was measured at abyssal depth. This movement feeds near-bottom water from the Scotia Sea continuously into the deep South Pacific Ocean, has a mean vector of 20.9 ± 5.3 cm s^{-1} towards 222° relative to true north and maximum velocities of 32 cm s^{-1} with an average temperature of −0.02 ± 0.06 °C. The countercurrent was also noted north of Livingston Island during the Dynamic Response and Kinematic Experiment (DRAKE) in 1979[16].

Material in the sediment traps was recovered from water depths at 965 m and 2,540 m; the samples are designated M 269-965 and M 269-2540, respectively. Chloroform for preservation was released into the collecting vessel during trap deployment from an imploding glass vial. Surface particulate matter was also collected at the mooring site on 25 January 1981 for 8 h. About 3 m^3 of sea-surface waters from the RV *Meteor's* contamination-free pumping system were continuously filtered through a 75-μm mesh sieve to concentrate enough material for individual component analyses; this sample is designated M 8101-38.

On recovery the sediment trap material and the surface particulate matter were split into 10 aliquots by pipetting from a suspension in filtered seawater which was kept homogenous by continuous agitation. To minimize bacterial degradation, splits were immediately poisoned with 100 p.p.m. $HgCl_2$ and frozen. Just before analysis, the samples were thawed and de-salted by repeated washings in distilled water, then they were freeze-dried. The wash water was retained for labile phosphorous determinations. The yields of 8 out of 10 splits gave total dry weights, estimated to be accurate to within 5 mg. These estimates were then used to calculate the total mass fluxes of 143 ± 1 g m^{-2} yr^{-1} at 2,540 m, 163 ± 2 g m^{-2} yr^{-1} at 965 m and 471 ± 6 g m^{-2} yr^{-1} at the surface. The measure for the mass flux at the surface is the product of the mean organic carbon fixation rate[15] multiplied by the bulk mass of the surface particulate matter divided by the concentration of organic carbon, and is considered a first approximation of the net bulk production. All individual component fluxes will be calculated from these bulk flux estimates.

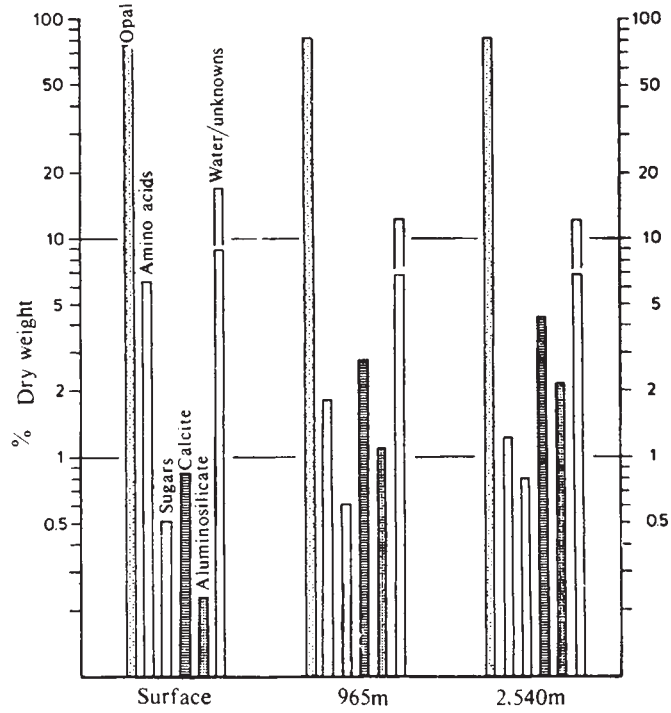

Fig. 1 Relative changes in major phase composition of particulate matter with water depth in the Drake Passage.

Individual splits were analysed for elemental and phase composition, amino acid, amino sugar and carbohydrate contents and foraminiferal counts, using methods described elsewhere[17]. In addition, hand-picked foraminifera were analysed for their stable isotope composition as described elsewhere[18]. Results of the major element and stable isotope compositions are listed in Table 1.

Most of the material collected in the traps, and virtually all of the surface particulate matter, was biogenic with a very minor portion of aluminosilicates. Figure 1 illustrates the relative changes in the major particulate phases with water depth. Whole individuals of diatoms, fragments and molds of crustaceans and tests of foraminifera were most abundant. The tests were almost exclusively of the left-coiling variety of the species *Globoquadrina pachyderma*. Faecal pellets were also common.

Quantitatively, diatomaceous debris is the dominant constituent as seen in the high SiO_2-content (Table 1, Fig. 1). Hereby the percentages listed refer to anhydrous SiO_2 only, thus the H_2O of diatomaceous opal, estimated to be between 6 and 9 wt%, may largely account for the unknown portion of the total biogenic matter.

The next most important phase is organic matter which shows a change from the surface particulates to the deep trap material in decreasing protein and labile phosphorus and increasing carbohydrate contents. Calcium carbonate and the aluminosilicate fractions increase in relative importance with water depth, obviously due to the more rapid disappearance of opal and

0028-0836/82/360145—03$01.00

Table 1 Major element and stable isotope composition of sediment trap material and surface plankton

	(wt%) de-salted and freeze-dried material								$\delta^{18}O$ (‰ PDB)	$\delta^{13}C$ (‰ PDB)
	C-total C-carb C-org	N-total	P-sum P-leach P-HCl P-total	Ash SiO_2	Ca-sol Ca-res	Mg-sol Mg-res	Al-sol Al-res	Ba-sol Ba-res	>300*	~200 ~125
M 8101-38, sea surface										
Split (1)	8.00	1.35	0.655	78.0	0.194	0.155	0.010	0.002	ND	ND
	ND	1.39	0.578	74.9	0.014	0.024	0.023	0.007		
	ND		0.015							
			0.077							
Split (8)	7.78	1.34	0.589	78.5	0.197	0.140	0.005	0.002	ND	ND
	0.14	1.32	0.513	75.5	0.016	0.022	0.021	0.003		
	7.12†		0.014							
			0.076							
M 269-965, 965 m depth										
Split (1)	3.36	0.48	0.064	86.4	0.832	0.067	0.005	0.023	3.26	0.74
	ND	ND	0.024	81.5	0.095	0.098	0.106	0.094	3.08	0.83
	ND		0.005						3.39	0.80
			0.041							
Split (8)	3.85	0.51	0.066	86.2	0.737	0.072	0.021	0.021	ND	ND
	0.33	ND	0.026	80.0	0.058	0.060	0.122	0.124		
	2.85†		0.007							
			0.041							
M 269-2540, 2540 m depth										
Split (1)	4.19	0.48	0.090	85.8	1.18	0.088	0.041	0.033	3.28	1.06
	ND	ND	0.046	79.7	0.152	0.110	0.198	0.045	3.44	0.67
	ND		0.008						3.04	0.76
			0.044							
Split (8)	3.49	0.42	0.102	86.7	1.38	0.096	0.048	0.034	ND	ND
	0.55	ND	0.064	78.4	0.167	0.122	0.223	0.076		
	2.76†		0.010							
			0.038							

In each column the sequence of numbers for one sample split refers to the sequence of components as listed in the column heading: N-total, duplicate Kjeldahl determinations; C-total, CO_2 liberated by heat combustion; C-carb, CO_2 liberated by phosphoric acid; C-org, CO_2 liberated by dichromate/sulphuric acid digestion; P-HCl, hydrochloric acid-soluble; P-leach, water soluble; P-total, after water leach by nitric/fluoric acid digestion; P-sum, water soluble plus total phosphorus (calculated); ash, after ignition at 400 °C for 2 h; sol, hydrochloric acid soluble; res, residual (not hydrochloric acid soluble); for analytical scheme see ref. 17. ND, not determined.

* Splits (3)(6); shell size in μm.

† C-org contents used in carbon budget of Table 2.

organic matter. This is evident when comparing the respective changes in component flux rates with water depth.

The total calcium carbonate flux (determined from Ca and CO_2 analyses) into the traps was 4.5 and 6.6 g m^{-2} yr^{-1}, respectively; whereas the *G. pachyderma* test flux (determined from test counts) was $\sim 10 \times 10^5$ individuals for each trap. For the test sizes 125, 200 and 300 μm, individual weights ranged from 1.1 to 8.9 μg with a mean test weight of 5.2 μg, thus when comparing both fluxes, it appears that *G. pachyderma* may account for the entire calcium carbonate flux.

The stable isotope values of *G. pachyderma* for three size fractions are also listed in Table 1. The tests in both traps showed mean $\delta^{18}O$ values of 3.25‰ PDB and appear unchanged during growth. This is in contrast to results from other neritic environments where, in general, for the same species the larger (older) shells are enriched in ^{18}O (ref. 19). The constant $\delta^{18}O$ values may be due to the rather small temperature variation within the euphotic zone of the study area. Depth migration during growth, if it occurs in the life cycle of *G. pachyderma*, does not lead the organism to encounter large temperature changes in circumpolar waters. The mean $\delta^{18}O$ value of 3.25‰ PDB indicates an equilibrium precipitation temperature of +1.8 °C based on the 'calcite' palaeotemperature equation of Epstein[20] and assuming −0.65‰ for the circumpolar surface water[21]. The calculated temperature is in good agreement with measured ones which we have recorded; that is +3.0 °C at the sea surface, −0.26 °C at 100 m, +1.44 °C at 203 m and +2.01 °C at 446 m of water depth (R. Wittstock, personal communication). The salinity varies over this same depth range between

Table 2 Organic carbon, nitrogen and phosphorus budgets of surface plankton and sediment trap material

	Sea surface M 8101-38	965 m depth M 269-965	2,540 m depth M 269-2540
	(μmol g^{-1} dry wt)		
Organic carbon	5,930	2,380	2,300
Amino acid carbon	2,895	713	531
Amino sugar carbon	46	42	40
Carbohydrate carbon	170	207	256
Carbon accounted for	52%	40%	36%
Organic nitrogen	964	357	321
Amino acid nitrogen	748	193	145
Amino sugar nitrogen	7.7	7.1	6.6
Ammonia nitrogen	83	33	25
Nitrogen accounted for	87%	65%	55%
Total phosphorus*	201	21	31
Water-soluble	176	8	18
HCl-soluble*	5	2	3
Insoluble	20	11	10
Phosphorus accounted for	100%	100%	100%

Amino acid carbon and nitrogen, sum of 22 individual amino acids; amino sugars, sum of galactosamine and glucosamine: carbohydrate carbon, sum of 11 hexoses; results of individual amino acid and sugar spectra will be published elsewhere (P.J.M. and G.L. in preparation).

* Organic + apatitic phosphorus, whereby HCl-soluble fraction may be considered apatitic[24].

Table 3 Mean annual production and flux rate estimates of individual biogenic components and aluminosilicates at the sea surface, at 965 m and 2,540 m of water depth at station M 269

Particulates	Sea surface M 8101-38	965 m depth M 269-965	2,540 m depth M 269-2540
		($g\ m^{-2}\ yr^{-1}$)	
Total mass flux	471	163	143
Organic carbon	36.5	5.41	4.78
Amino acid carbon	16.4	1.39	0.91
Carbohydrate carbon	0.96	0.40	0.44
Amino sugar carbon	0.26	0.08	0.07
Organic nitrogen	6.36	0.81	0.64
Amino acid nitrogen	4.93	0.44	0.29
Ammonia nitrogen	0.55	0.075	0.050
Amino sugar nitrogen	0.05	0.016	0.013
Organic phosphorus			
Water soluble	2.57	0.041	0.079
Insoluble	0.29	0.057	0.046
Silica, anhydrous	354	132	113
Calcium carbonate	5.5	4.5	6.6
Barite	0.06	0.36	0.23
Aluminosilicates	1.08	1.79	3.00
Al_2O_3	0.20	0.35	0.57
MgO	0.18	0.21	0.27
CaO	0.10	0.17	0.32

Organic phosphorus (insoluble), P-total minus P-hydrochloric acid soluble; calcium carbonate, mixed Ca–Mg–carbonate probably also containing $SrCO_3$; barite, soluble plus residual barium plus stoichiometric SO_4; aluminosilicates, sum of residual oxides plus $3\times(Al_2O_3)$ as aluminosilicate SiO_2, flux rates do not include quartz-SiO_2; the individual component fluxes are calculated by averaging the compositions.

33.7 and 33.5‰ S, therefore our data indicate that *G. pachyderma* precipitates its tests close to isotopic equilibrium. The carbon isotope values also do not vary with shell size and thus do not show the 'normal' trend of ^{13}C enrichment with increasing age[19], again the rather homogeneous water column properties seem responsible for this low variability in the stable carbon isotope signature of *G. pachyderma*.

Dramatic qualitative and quantitative changes with water depth were observed for the organic matter fraction (Table 2). Whereas in surface plankton 52% of the total organic carbon may be accounted for as being tied up in polypeptides, proteins and polysaccharides, these portions decrease with depth to 40% and 36%, respectively. The non-characterized fraction probably contains hydrocarbons, wax esters and other lipid material as well as 'humic matter'; its proportion increases with depth from ~50 to ~65% of the total organic carbon pool.

Because only $\ll 1\ \mu mol\ g^{-1}$ of ammonia-N could be contained in the aluminosilicate fraction as fixed NH_3 (ref. 22), we assume that all nitrogen is organically bound. The free ammonia-N listed in Table 2 is also organically bound but is liberated from the protein fraction during hydrolysis.

The decrease in amino yield and the increase in carbohydrate contents with water depth reflect the preferential degradation of proteinaceous material[23]. This is supported by a decrease in both amino acid-C and amino acid-N, whereas the relative increase in the non-characterized organic nitrogen fraction might reflect a pronounced abundance of nucleic acid bases and/or 'humic material'. Amino sugars on the other hand, comprise a relatively stable fraction of both organic-C and organic-N at all depths, indicating that they may be derived from poorly degradable chitinaceous matter.

For phosphorus we attempted partitioning by a methodology based on fractional solubilization. This approach explains why we account for the entire phosphorus budget. Hereby the water-soluble portion probably represents very labile organic phosphorus compounds such as ATP and related energy storage compounds and nucleic acids, released from living cells. We then defined a small fraction of phosphorus, soluble in hydrochloric acid, which could come from apatitic biogenous skeletons[24]. Consequently, the calculated difference between P-sum minus P-HCl and P-leach represents an insoluble organic phosphorus fraction such as phospholipids from cell walls or similar tissue structures. The relative increase of this fraction from 10% at the sea surface to ~40% at depth also indicates it to be of a more refractory nature.

We may now compare flux rate changes of organic phases with mineral phases during transit through the water column (Table 3), because ultimately, fractionation resulting from such differential flux rates transforms surface particulate matter into bottom sediments. From Table 3, four types of biogeochemical regeneration can be differentiated. (1) Labile organic phosphorus is the most rapidly recycled; only <5% of that fraction escapes recycling within near-surface waters and reaches depths of ~1,000 m, below which its flux remains essentially constant. (2) Polypeptides, presumably proteinaceous material of surface plankton are at first rapidly recycled between the surface and ~1,000 m of depth and thereafter at a slower rate. This exponential degradation is seen in changes of amino acid-C, amino acid-N and ammonia-N fluxes; it essentially affects the entire particulate nitrogen pool. (3) Fluxes of skeletal silica, polysaccharides, amino sugars and insoluble organic phosphorus show a slight tendency of refractory chemical behaviour which is marked by imperceptibly small flux rate changes in deep water. This is not surprising, as all are 'residual' components of biogenic matter: opal of diatom tests, carbohydrates and insoluble phosphorus of cell walls and amino sugars of chitinaceous skeletons. (4) Finally, the behaviour of calcium carbonate, barite and aluminosilicates cannot be adequately assessed from our flux data, because their sources are not restricted to surface waters of the same region as indicated by the deep countercurrent. Therefore, the bulk production rate assumed for the surface is a poor estimate. All three components of this group may have sources farther to the east of the sampling site and thus are not included in our production rate estimate from surface particulate matter. Similarly, aluminosilicates are advected horizontally and vertically throughout the water column, and the deeper the traps are deployed, the larger the aluminosilicate fluxes will be. But at least our flux data indicate that calcium carbonate, barite and aluminosilicates are very refractory and will undergo little, if any, recycling in the water column below ~1,000 m due to rapid transit.

This work was supported by the Deutsche Forschungsgemeinschaft and the US Office of Naval Research through grant N00014-79-C-0004, Project NR083-1026 to Oregon State University. We thank especially B. von Bodungen and R. Wittstock for help in deployment and recovery of the moorings in the Drake Passage. This is contribution no. 394 from the Sonderforschungsbereich 95, University of Kiel.

Received 5 April; accepted 7 June 1982.

1. Schrader, H.-J. *Science* **174,** 55–57 (1971).
2. Hinga, K. R., Sieburth, J. & Heath, G. R. *J. mar. Res.* **37,** 557–579 (1979).
3. Cobler, R. & Dymond, J. *Science* **209,** 801–802 (1980).
4. Suess, E. *Nature* **288,** 260–263 (1980).
5. Thunell, R. & Honjo, S. *Mar. Geol.* **40,** 237–253 (1981).
6. Honjo, S., Manganini, S. J. & Cole, J. J. *Deep-Sea Res.* **29,** 609–625 (1982).
7. Deuser, W. G., Ross, E. H. & Anderson, R. F. *Deep-Sea Res.* **28,** 495–505 (1981).
8. Knauer, G. A., Martin, J. H. & Bruland, K. W. *Deep-Sea Res.* **26,** 97–108 (1979).
9. Starecinic, N. *J. mar. Res.* (in the press).
10. Wakeham, S. G. *et al. Nature* **286,** 798–800 (1980).
11. Deuser, W. G. & Ross, E. H. *Nature* **283,** 364–365 (1980).
12. Knauer, G. A. & Martin, J. H. *Limnol. Oceanogr.* **26,** 181–186 (1981).
13. Urrere, M. A. & Knauer, G. A. *J. Plankton Res.* **3,** 3–19 (1981).
14. Zeitzschel, B., Uhlmann, L. & Diekmann, P. *Mar. Biol.* **45,** 285–288 (1978).
15. Tilzer, M. & von Bodungen, B. *Berichte aus dem Institut für Meereskunde* No. 80 (1981).
16. Whitworth, T., Nowlin, W. D. Jr & Worley, S. J. *J. Phys. Oceanogr.* (in the press).
17. Suess, E. & Ungerer, C. A. *Oceanol. Acta* **4,** 151–160 (1980).
18. Berger, W. H. & Killingley, J. S. *Science* **197,** 563–566 (1977).
19. Berger, W. H., Killingley, J. S. & Vincent, E. *Oceanol. Acta* **1,** 203–216 (1978).
20. Epstein, S., Buchsbaum, H. A., Lowenstamm, H. A. & Urey, H. C. *Bull. geol. Soc. Am.* **64,** 1315–1325 (1953).
21. Craig, H. & Gordon, L. I. *Stable Isotopes in Oceanographic Studies* (ed. Tongiorgi, E.) 9–130 (Consiglio Nazionale delle Richerche, Rome, 1965).
22. Müller, P. J. *Geochim. cosmochim. Acta* **41,** 765–776 (1977).
23. Handa, N. & Yanagi, K. *Mar. Biol.* **4,** 197–207 (1969).
24. Black, C. A. *Methods of Soil Analysis* Pt II, 1038–1040 (American Society of Agronomy, Madison, 1965).